Vietnam Journal of Science and Technology ***62*** *(4) (2024) 725-736*

doi:10.15625/2525-2518/17254

2K/UV dual-curable acrylate epoxy/SiO_2 nanocomposite coatings: crosslinking and mechanical properties

Nguyen Ngoc Linh[1, 2], Dang Thi My Linh[3], Nguyen Tuan Anh[3], Vu Quoc Trung[4], Nguyen Thien Vuong[1, 3, *]

[1]*Graduate University of Science and Technology, Vietnam Academy of Science and Technology, 18 Hoang Quoc Viet, Cau Giay, Ha Noi, Viet Nam*

[2]*Faculty of Pharmacy, Thanh Do University, Kim Chung, Hoai Duc, Ha Noi, Viet Nam*

[3]*Institute for Tropical Technology, Vietnam Academy of Science and Technology, 18 Hoang Quoc Viet, Cau Giay, Ha Noi, Viet Nam*

[4]*Faculty of Chemistry, Hanoi National University of Education, 136 Xuan Thuy, Cau Giay, Ha Noi, Viet Nam*

[*]Emails: *vuongvast@gmail.com*

Received: 2 July 2022; Accepted for publication: 15 August 2022

Abstract. This work aimed to enhance the adhesion of photocurable acrylate epoxy/SiO_2 nanocomposite coating by adding a crosslinking agent polyisocyanate Desmodur N75 (N75) to make a 2K/UV dual-curable paint formulation. The obtained results showed that the presence of the curing agent N75 slightly reduced the conversion efficiency of acrylate groups during the UV curing process. The analysis of mechanical properties indicated that the coating achieved the optimal mechanical properties at the N75 content of 5 wt.%. The gel fraction, swelling degree, adhesion to wood and steel, relative hardness, impact resistance, and abrasion resistance reached 97.22 %, 310.05 %, 0.1, 0.94, 90 Kg.cm, and 178 L/mil, respectively. FESEM analysis showed that the paint film was fairly homogeneous and tightly structured. The reactions of components of BGDM, HDDA, I184, N75 and nano-SiO_2 in the 2K/UV dual-curable acrylate epoxy/SiO_2 nanocomposite coatings were described.

*Keywords: a*crylate epoxy, polyisocyanate, SiO_2 nanoparticles, mechanical properties, 2K/UV dual-cure coating.

Classification numbers: 2.5.3, 2.9.4.

1. INTRODUCTION

The UV-cured coatings exhibit many advantages over other conventional coatings, such as better physico-mechanical properties, higher chemical resistance and weathering durability [1, 2]. In particular, the processing technology is eco-friendly due to being conducted at room temperature and not releasing toxic organic waste [3, 4]. Because of the rapid curing process and

remarkable properties as mentioned before, the coatings have been widely applied in paint industry such as wood flooring [5, 6]. However, there are some limitations to UV curing resin, for instance, high shrinkage (up to 15 %) and low adhesion in some particular cases [7,8]. To overcome this challenge, 3 effective methods can be used: (i) reinforcement with inorganic fillers [9, 10]; (ii) increasing the curing density [11]; and (iii) choosing ingredients with an appropriate structure [12, 13]. Nano-silica (nano-SiO_2) is an excellent inorganic filler to reinforce polymer materials, especially organic coatings. Besides, many studies have shown that nano-SiO_2 can improve the thermal resistance [4, 14], weathering resistance [15, 16], and alkaline or acidic resistance of the coatings [17, 18], etc. Despite this, inorganic and organic fillers supplemented to the paint formulation can participate in the curing reactions [19,20], forming a tight organic–inorganic hybrid structure [21 - 23]. To increase the curing density of the UV curing coatings, the curing agent polyisocyanate was added to create a 2K/UV dual curable paint system. As a consequence, the paint films have a tight structure with outstanding mechanical and weathering resistance [24].

In our previous work [4], we investigated the characteristics and properties of UV curing nanocomposites based on bisphenol A glycerolate dimethacrylate, 1,6-hecxanediol diacrylate, and reinforcing filler (nano-SiO_2) using 1-hydroxy-cyclohexyl-phenyl-ketone as a photo-initiator. The results showed that the nano-SiO_2 reduced the conversion efficiency of the acrylate/metacrylate double bond since the nano-SiO_2 can absorb and scatter UV light, leading to the low UV curing efficiency. The coating with 2.5 wt.% nano-SiO_2 has outstanding mechanical properties (impact resistance, falling sand abrasion resistance) and thermal resistance compared to the neat coating. However, the adhesion of the coating was low, thereby restricting its practical application. In this study, the curing agent polyisocyanate was added to the paint formulation to make a dual curing resin system, aiming to increase the adhesion of the paint coating.

2. MATERIALS AND METHODS

2.1. Materials

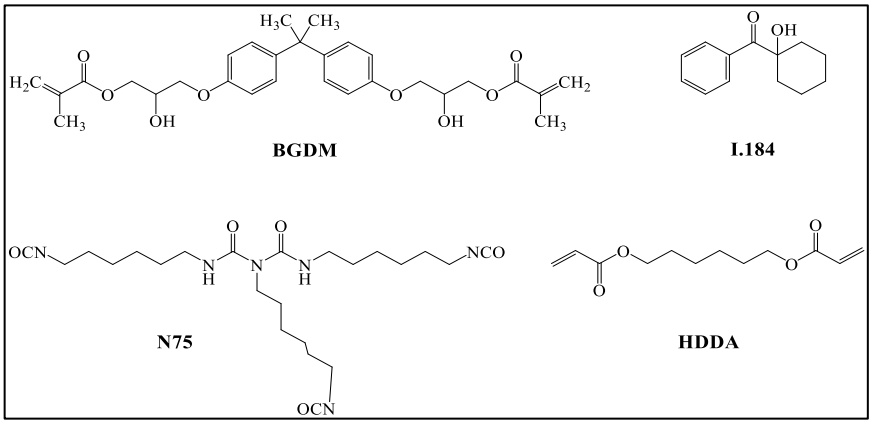

Figure 1. Chemical formula of BGDM, HDDA, I.184 and N75.

Bisphenol A glycerolate dimethacrylate (BGDM) and 1,6-hecxanediol diacrylate 80 % (HDDA) were ordered from Sigma-Aldrich. The photo-initiator 1-hydroxy-cyclohexyl-phenyl-ketone, Irgacure 184 (I.184) was provided by CIBA (Merck). Desmodur N75 polyisocyanate

(N75) liquid (75 wt.%) containing 17 wt.% of isocyanate group content, used as a crosslinking agent, was provided by Bayer. Their structures were described in Figure 1.

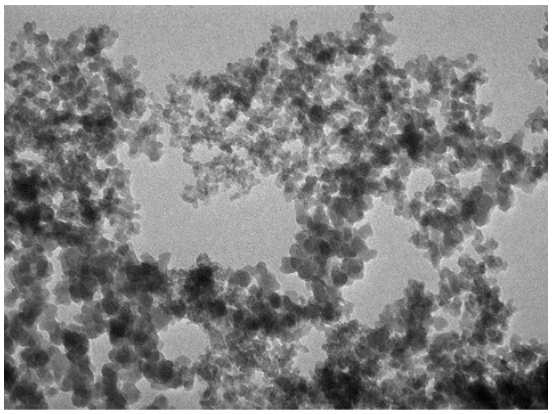

Figure 2. TEM image of nano-SiO_2 particles as-synthesized from rice husk ash.

The nano-SiO_2 particles used were about 20 nm in size and were synthesized according to the method presented in our previous work [17] (Figure 2).

2.2. Preparation of coating samples

The coating samples with various N75 contents from 0 to 10 wt.% (by weight on total resin of BGDM&HDDA) were prepared with coating formulation shown in Table 1. The ratio of BGDM/HDDA/I184/nano-SiO_2 = 55/45/3/2.5 was found to be the optimal paint formulation from our previously works [3, 4, 16].

Table 1. Paint formulations with different contents of N75.

Material	Content of N75 (wt.%)				
	0	2.5	5	7.5	10
N75	0	0.05	0.10	0.15	0.20
BGDM	1.1	1.1	1.1	1.1	1.1
HDDA	0.9	0.9	0.9	0.9	1.1
I.184	0.06	0.06	0.06	0.06	0.06
Nano-SiO_2	0.05	0.05	0.05	0.05	0.05

To fabricate the nanocomposite coatings, firstly nano-SiO_2 particles were dispersed in HDDA using a TP-25 ultrasonic bath (Switzerland) during 3 hours. After that, BGDM resin and I184 were added to the mixture, followed by further sonication for 30 minutes. Finally, the curing agent N75 was added to this as-prepared mixture under mechanical stirring for 10 minutes.

Thin films were then coated on different substrates, such as KBr pellets, Teflon, Incense wood, CT3 steel sheets and glass plates for further evaluations. To control the thickness of the coating samples, a Quadruple Film Applicator (Enrichen model 360) or a Spiral Film Applicator (Erichsen model 358) was used.

For UV-curing process, a UV curing device (model F300S, USA) was used with a medium-pressure mercury lamp (250 mW/cm^2) at 25 ^oC. To estimate the curing time under the UV-light,

the web rates from 5 to 40 m/s were selected. Thus, the UV exposure time of the paint film was calculated based on the web rate. For example, for a web rate of 40 m/s, the exposure time was 0.15 s.

The coating samples after UV curing were dried under room conditions for 4 days before testing. The average thickness of the coating samples was about 30 μm.

2.3. Characterization

2.3.1. IR characterization

The conversion of reactive functional groups during the curing process was monitored by quantitative IR analysis using NEXUS 670 FTIR spectroscopy (Nicolet). The conversion of acrylate double (AD) bond was evaluated by the change in the characteristic peak at 983 cm^{-1}. The characteristic peak of the benzene ring at 1510 cm^{-1} was used as an internal standard [4]. The conversion of isocyanate groups was tracked by the change in optical density of the characteristic peak at 2272 cm^{-1} [24].

The optical density (D) of the groups was estimated according to the following formula:

$$D = \log (I_0/I) = \log [1+H/(100-U)] \quad (1)$$

The relationship between I_0 and I with H and U is shown in Figure 3, where H and U were calculated using the software of FTIR spectroscopy.

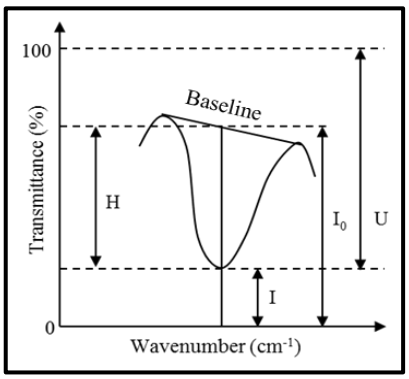

Figure 3. Relationship between I_0 and I with H and U.

The remaining acrylate group was calculated as follows:

$$\text{Remaining acrylate group (\%)} = [(D_{983\ cm\text{-}1}/D_{1510\ cm\text{-}1})_t/(D_{983\ cm\text{-}1}/D_{1510\ cm\text{-}1})_0] \times 100 \quad (2)$$

where: D_0 and D_t are the optical densities of the groups before and after curing.

2.3.2. Gel fraction, swelling degree

The gel fraction (GF) and swelling degree (SD) of the paint films were evaluated using the Soxhlet method in accordance with the ASTM D2765 standard [4].

2.3.3. Microstructural analysis

The morphology and size of nano-SiO_2 particles and nanocomposite coatings were observed using a Field emission scanning electron microscope, S 4800 (FE-SEM) and Transmission Electron Microscope (TEM) (Japan).

2.3.4. Measurement of mechanical properties

Various mechanical parameters, such as adhesion, impact resistance and abrasion resistance of the coatings were measured according to the methods and standards presented in previous papers [14, 24]. Specifically, the adhesion was measured according to the ISO 2409 with an Elcometer Cross Hatch Cutter (England), the impact resistance was tested according to the ISO 6272 using an impact tester (model 304, Germany) [24]. The abrasion resistance was performed in accordance with the ASTM D968 standard [14].

3. RESULTS AND DISCUSSION

3.1. Crosslinking characteristics of 2K/UV dual-cure nanocomposite coating

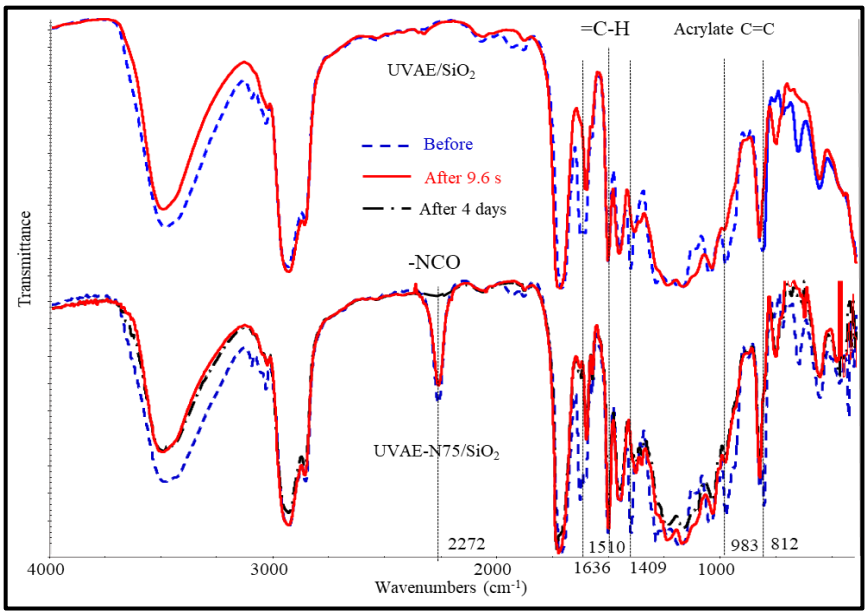

Figure 4. IR spectra of UV-cure acrylate epoxy/SiO_2 nanocomposite coating (UVAE/SiO_2) and 2K/UV dual-cure acrylate epoxy/SiO_2 nanocomposite coating with 5 wt.% N75 (UVAE-N75/SiO_2) before and after crosslinking.

Crosslinking characteristics of the coatings were investigated based on the conversion of the reactive functional groups and changes in their GL and SD values [4, 5, 24]. IR spectra of 2K/UV dual-cure acrylate epoxy/SiO_2 nanocomposite coating (UVAE-N75/SiO_2) based on Bisphenol A glycerolate dimethacrylate, 1,6-hecxanediol diacrylate, 1-hydroxy-cyclohexyl-phenyl-ketone, polyisocyanate Desmodur N75 (5 wt.%) and nano-SiO_2 before and after crosslinking are presented in Figure 4. IR spectra of UV-cure acrylate epoxy/SiO_2 nanocomposite coating (without N75) (UVAE/SiO_2) are also presented in this figure for reference. Some characteristic vibrations in the IR spectra of the above coatings are shown in Table 2.

As can be seen in Figure 4 and Table 2, all characteristic peaks of AD bonds at 1636 cm^{-1}, 1409 cm^{-1}, 983 cm^{-1}, and 812 cm^{-1} decreased after exposure to UV. Among those, the peak at 983 cm^{-1} had a clear rule for reduction and was not overlapped by other peaks, hence it was chosen to evaluate the conversion of acrylate groups. The conversion of the isocyanate groups was established by the optical density degradation of the peak at 2272 cm^{-1}. The quantitative analysis of the conversion of acrylate and isocyanate groups is shown in Figure 5.

Table 2. Main characteristic vibrations in IR spectra of nanocomposite before and after crosslinking process.

ν (cm^{-1})	Characteristic vibration	UVAE-SiO_2		UVAE-N75-SiO_2		Comment
		Before	After 9.6 s	Before	After 9.6 s	
3530-3460	ν O–H alcohol, acid	+	+	+	+	Overlap
3398-3300	ν N–H amide, amine			+	+	Overlap
3100	ν =C–H mono-substituted benzene	+	+	+	+	No change
2960, 2850	ν C–H (CH_3, CH_2)	+	+	+	+	No change
2272	ν N=C (–N=C=O)			+	+	Decrease clearly
1730	ν C=O ester	+	+	+	+	No change
1636	ν C=C acrylate	+	+	+	+	Decrease, overlap
1609	ν C=C benzene	+	+	+	+	Overlap
1532-1518	δ N–H amide			+	+	Overlap
1510	ν C=C benzene	+	+	+	+	No change
1460, 1378	δ C–H (CH_3, CH_2)	+	+	+	+	Decrease
1250-1086	ν C–O– ester, ether	+	+	+	+	Overlap
983	$\delta_{rocking}$ =CH–conjugated double bonds	+	+	+	+	Decrease clearly
830, 756	δ_{nmf} C–H disubstituted benzene 1,4	+	+	+	+	Overlap
812	$\delta_{rocking}$ $=CH_2$ acrylate	+	+	+	+	Decrease, overlap

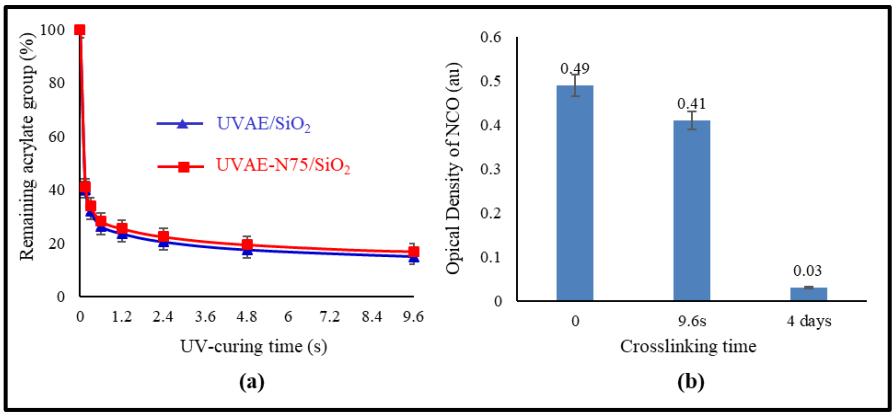

Figure 5. Conversion of reactive functional groups in the coatings.

In addition, as shown in Figure 5, the AD bonds decreased rapidly from 0 to 0.3 s of UV irradiation and were gradually slowly reduced in the range of 0.3-9.6 s of UV exposure. The conversion of AD bonds in the coating containing 5 wt.% N75 (UVAE-N75/SiO_2) degraded more slightly compared to the coating without N75 (UVAE/SiO_2). After 9.6 s of UV exposure,

the remaining content of acrylate was 16.9 % for UVAE-N75/SiO_2 film and 14.9 % for UVAE/SiO_2 film. The optical density of the characteristic absorbance of isocyanate groups (–CNO) decreased from 0.49 to 0.41 au, but after 4 days, this value remained at 0.04 au (Figure 4b). It means that almost of the –CNO groups had been conversed.

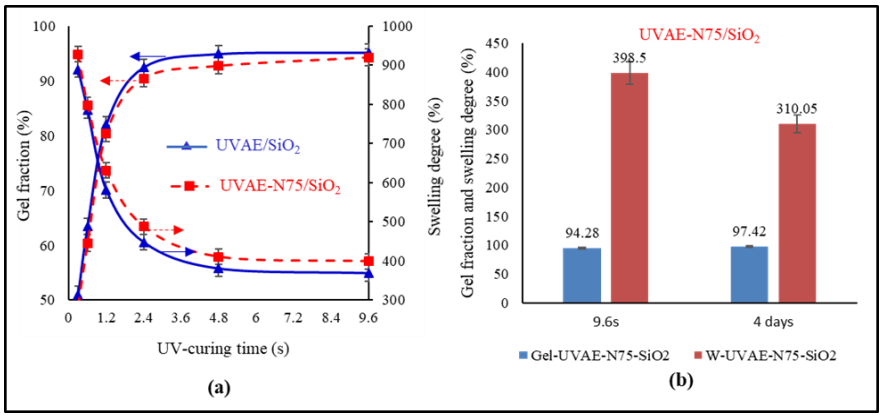

Figure 6. Evolution of GF and SD values for nanocomposite coatings.

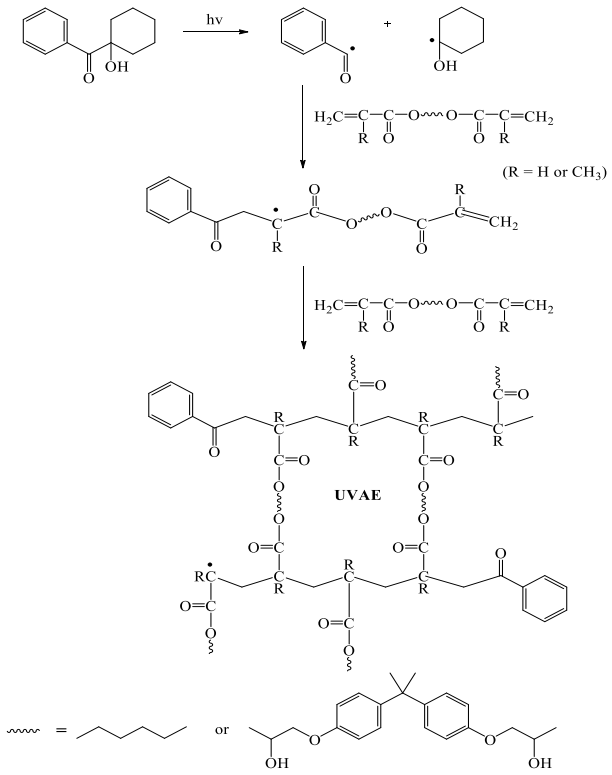

Scheme 1. UV curing reaction progress of BGDM, HDDA and I184 [1].

Figure 6 presents the values of GF and SD of UVAE-N75/SiO_2 and UVAE/SiO_2coatings. In Figure 6a, during the curing process, the GF and SD values decreased quickly in the first 2.4 s of UV exposure, then the rate slowed down. After 9.6 s of UV exposure, the GF and SD of

UVAE-N75/SiO_2 film reached 94.28 % and 398.5 %, respectively, whilst the corresponding values of UVAE/SiO_2 films were 95.18 % and 368.55 %. So, after 9.6 s of UV exposure, the GF of UVAE-N75/SiO_2 film was lower and its swelling degree was higher than those of UVAE/SiO_2 film, correspondingly. After 4 days, the GF of the UVAE-N75/SiO_2 film increased from 94.28 to 97.42 and the SD decreased from 398.5 to 310.05 % (Figure 6b).

Accordingly, the addition of 5 wt.% polyisocyanate agent N75 to the UV-curable resin system not only alleviated the conversion of AD bonds, but also reduced the GF and increased the SD values (after 9.6 s of UV irradiation). However, after 4 days of curing, this paint film had a higher GF and a lower SD compared to the coating without N75. The presence of N75, which prevented the initiating free radicals from approaching the acrylate groups, can be a reason for the slightly lower conversion of AD bonds and lower GF as well as higher SD after 9.6 s of UV exposure. The lower GF and SD values were possibly caused by the lower participation of the N75 agent during the curing process. Evidently, its characteristic IR peaks were slightly reduced from 0.49 to 0.41. Since the N75 agent continued to react with –OH groups in the BGDM chain, the GF increased and the swelling degree decreased noticeably. The ano-SiO_2 not only played the role of a reinforcing filler but also reacted with the isocyanate groups.

In addition, during the crosslinking process, the content of –NCO groups decreased due to the reaction with the OH groups of BGDM to form urethane structures (–NHCOO–). In the presence of nano-SiO_2, the NCO groups can also react with the –OH groups on the surface of the nanoparticles [21] leading to a reduction of the –NCO groups and the formation of an inorganic-organic hybrid structure and an increase of crosslinking density of the coating. Based on the above obtained experimental data, the 2K/UV dual-cure reaction of BGDM, HDDA and N75 in the presence of nano-SiO_2 can be described as follows (Scheme 1 and Scheme 2):

3.2. Effect of curing agent N75 on the properties of 2K/UV dual-cure nanocomposite coating

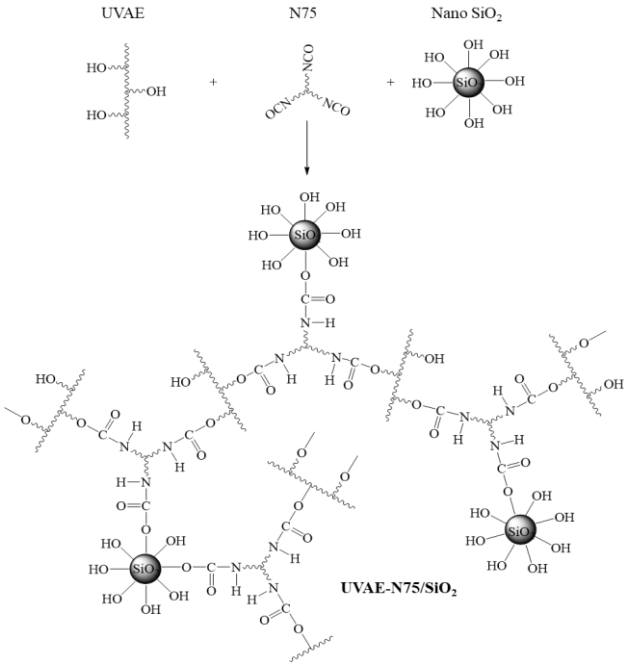

Scheme 2. Crosslinking reaction of Desmodur N75 polyisocyanate with –OH groups of BGDM and nano-SiO_2 [21].

Table 3. Effect of N75 on the GF, SD and mechanical properties of 2K/UV dual-curable nanocomposite coating.

N°	Characteristic	Content of N75 (wt.%)				
		0	2.5	5	7.5	10
1	Gel Fraction (GF), %	94.93	96.21	97.22	97.28	97.33
2	Swelling Degree (SD), %	378.52	350.24	310.05	295.78	290.65
3	Adhesion (on Incense wood), Level	3	1	0	0	0
4	Adhesion (on CT3 Steel), Level	3	2	1	1	1
5	Relative Hardness	0.89	0.92	0.94	0.94	0.93
6	Impact resistance, Kg.cm	40	70	90	80	65
7	Abrasion resistance, L/mil	158	165	178	172	160

The GF, SD values and mechanical properties of the coating with different contents of N75 (0 - 10 wt.%) are illustrated in Table 3.

The data obtained showed that as the content of the curing agent N75 increased from 0 to 5 %, the GF, the adhesion to wood and steel, the relative hardness, the impact resistance, and the falling sand abrasion resistance all increased, whilst the SD obviously decreased. The values were 97.22 %, 0, 1, 0.94, 90 Kg.cm, 178 L/mil and 310.05 %, respectively. When the content of N75 continued to increase by up to 10 %, the GF and the SD changed negligibly, the adhesion to wood and steel remained as well as the relative hardness remained, and the impact resistance and the abrasion resistance were both reduced.

As a consequence, the best mechanical property of the coating was achieved when 5 wt.% of curing agent N75 was used. This finding could be explained by the fact that the coating was cured more effectively with a more tightly structure when 5 wt.% N75 was used. However, at a higher content of N75, the compact structure of nanocomposite coating could be deteriorated significantly.

Figure 7 shows the FE-SEM images of UV-cure acrylate epoxy/SiO_2 nanocomposite coating (UVAE/SiO_2) and 2K/UV dual-curable acrylate epoxy/SiO_2 nanocomposite coating with 5 wt.% N75 (UVAE-N75/SiO_2).

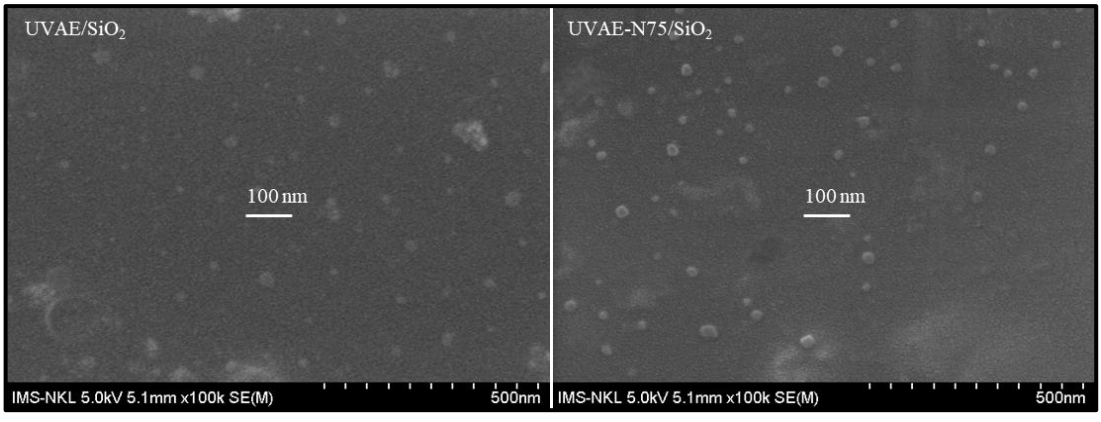

Figure 7. FE-SEM images of UV-cure acrylate epoxy/SiO_2 nanocomposite coating (UVAE/SiO_2) and 2K/UV dual-curable acrylate epoxy/SiO_2 nanocomposite coating with 5 wt.% of N75 (UVAE-N75/SiO_2).

Clearly, both coatings had a tight structure, the nano-SiO_2 particles were relatively well-dispersed. The dispersion ability of the nano particles was independent of the presence of the curing agent N75.

4. CONCLUSIONS

Crosslinking, mechanical properties and microstructure of 2K/UV dual-curable acrylate epoxy/SiO_2 nanocomposite coatings have been evaluated under various fabricating conditions.

The presence of the curing agent N75 alleviated the conversion efficiency of AD bonds during the curing process. The highest mechanical properties of the coatings were obtained when 5 wt.% of N75 curing agent was used. The highest values of GF, SD, adhesion (to wood and steel substrates), relative hardness, impact resistance, abrasion resistance were 97.22 %, 310.05 %, 0, 1, 0.94, 90 Kg.cm, 178 L/mil, respectively.

The FESEM data indicated that nano-SiO_2 particles were homogeneously dispersed into the UV cured coating, giving rise to its tight structure. In addition, the 2K/UV dual-curable reaction of acrylate epoxy/SiO_2 nanocomposite coatings based on BGDM, HDDA, I184, N75, and nano-SiO_2 have been described in detail.

Acknowledgments. The authors thank the Graduate University of Science and Technology - VAST for the financial support (GUST.STS.ĐT 2020-HH06).

CRediT authorship contribution statement. Nguyen Ngoc Linh: Investigation, Funding acquisition, Writing - original paper. Dang Thi My Linh: Investigation. Nguyen Tuan Anh: Review & editing. Vu Quoc Trung: Formal analysis. Nguyen Thien Vuong: Writing-review & editing.

Declaration of competing interest. The authors declare that they have no known competing financial interests or personal relationships that could have appeared to influence the work reported in this paper.

REFERENCES

1. Nguyen-Tri P., Nguyen T. V. - Radically curable nanobased coatings (chapter 10), In: Phuong Nguyen Tri, Sami Rtimi and Claudiane Ouellet-Plamondon (Eds), Nanomaterials Based Coatings, Elsevier, 2019, pp. 1-35. https://doi.org/10.1016/B978-0-12-815884-5.00010-7.
2. Nguyen T. V., Nguyet H. M., Linh D. T. M. - Influence of organic UV absorber on the accelerated weathering stability of UV curing coating based on acrylate urethane resin, Vietnam J. Chem. **58** (2) (2020) 173-179. https://doi.org/10.1002/vjch.201900127.
3. Le X. H., Nguyen T. V., Le M. T., Nguyen T. V. Trieu - Study of photocrosslinking reaction of the resin system on the base of copolymer of tung and soyabean oils, methyl methacrylate, styrene, Vietnam J. Sci. Tech. **48** (3A) (2010) 150-157.
4. Nguyen N. L., Dang T. M. L., Nguyen T. A., Ha H. T., Nguyen T. V.- Study on Microstructure and Properties of the UV Curing Acrylic Epoxy/SiO_2 Nanocomposite Coating. Journal of Nanomaterials, 2021.https://doi.org/10.1155/2021/8493201.
5. Do T. V., Ha M. N., Nguyen T. A., Ha H. T., Nguyen T. V. - Crosslinking, Mechanical Properties, and Antimicrobial Activity of Photocurable Diacrylate Urethane/ZnO-Ag Nanocomposite Coating, Adsorption Science & Technology, 2021. https://doi.org/10.1155/2021/7387160.

6. Brito M. de, Allonas X., Croutxé-Barghorn C., Palmieri M., Alig I. - Kinetic study of photoinduced quasi-simultaneous interpenetrating polymer networks, Progress in Organic Coatings **73** (2 - 3) (2012) 186-193. https://doi.org/10.1016/j.porgcoat.2011.10.014.
7. Talita A. T. C., Aline de A. N., Ingrid K. B. dos S., Amanda R. P. de R., Eduardo M. da S. - Characterization of low-shrinkage dental composites containing methacrylethyl-polyhedral oligomeric silsesquioxane (ME-POSS), Journal of the Mechanical Behavior of Biomedical Materials **90** (2019) 566-574. . https://doi.org/10.1016/j.jmbbm.2018.10.028.
8. Lee S. J., Kawashima S., Kim K. J., Woo S. K., Won J. P. - Shrinkage characteristics and strength recovery of nanomaterials-cement composites, Composite Structures **202** (2018) 559-565. https://doi.org/10.1016/j.compstruct.2018.03.003.
9. Tafesse M., Kim H. K. - The role of carbon nanotube on hydration kinetics and shrinkage of cement composite, Composites Part B: Engineering **169** (2019) 55-64. https://doi.org/10.1016/j.compositesb.2019.04.004.
10. Bhanu P., Ravi K. G., Bhuvnesh B., Meetu N. - Modeling based experimental investigation on polymerization shrinkage and micro-hardness of nano alumina filled resin based dental material, Journal of the Mechanical Behavior of Biomedical Materials **99** (2019) 86-92. https://doi.org/10.1016/j.jmbbm.2019.06.026.
11. M. Sangermano, W. Carbonaro, G. Malucelli, A. Priola, UV-Cured Interpenetrating Acrylic Epoxy Polymer Networks: Preparation and Characterization, Macromol. Mater. Eng. **93** (2008), 515-520. https://doi.org/10.1002/mame.200800020.
12. Rocco C., Karasu F., Croutxé-Barghorn C., Allonas X., With de G. - Highly-interpenetrated and phase-separated UV-cured interpenetrating methacrylate–epoxide polymer networks: Influence of the composition on properties and microstructure, Materials Today Communications **6** (2016) 17-27. https://doi.org/10.1016/j.mtcomm.2015.11.004.
13. Sufyan G., Pekka K. V., David C. W., Lippo V. J. L. - Effect of nanofiller fractions and temperature on polymerization shrinkage on glass fiber reinforced filling material, Dental Materials **24** (5) (2008) 606-610. https://doi.org/10.1016/j.dental.2007.06.020.
14. Lee S. J., Kawashima S., Kim K. J., Woo S. K., Won J. P. - Shrinkage characteristics and strength recovery of nanomaterials-cement composites, Composite Structures **202** (2018) 559-565. https://doi.org/10.1016/j.compstruct.2018.03.003.
15. Le T. T., Nguyen T. V., Nguyen T. A., Nguyen T. T. H., Hoang T., Tran D. L., Dinh D. A., Nguyen T. M., Le T. L. - Thermal, mechanical and antibacterial properties of water-based acrylic polymer/SiO_2-Ag nanocomposite coating, J. Mater. Chem. Phys. **232** (2019) 362-366. https://doi.org/10.1016/j.matchemphys.2019.05.001.
16. Nguyen T. V., Nguyen T. A., Nguyen T. H. - The Synergistic Effects of SiO_2 Nanoparticles and Organic Photostabilizers for Enhanced Weathering Resistance of Acrylic Polyurethane Coating, J. Compos. Sci. **4** (2020) 23.https://doi.org/10.3390/jcs4010023.
17. Bui T. M. A., Nguyen T. V., Nguyen T. M., Hoang T. H., Nguyen T. T. H., Lai T. H., Tran T. N., Nguyen V. H., Hoang V. H., Le T. L., Tran D. L., Dang T. C., Vu Q. T., Nguyen T. P. - Crosslinking mechanism, mechanical properties and weathering degradation of acrylic polyurethane nanocomposite coating reinforced by SiO_2 nanoparticles issued from rice husk ash, J. Mater. Chem. Phys. **241** (2020) 122445. https://doi.org/10.1016/j.matchemphys.2019.122445.

18. Nguyen T. M., Bui T. M. A., Nguyen T. V. - Acid and alkali resistance of Acrylic polyurethane/R-SiO_2, Vietnam Journal of Chemistry **58** (1) (2020) 67-73. https://doi.org/10.1002/vjch.2019000124.
19. Hoang T. H. T., Hoang T. H., Nguyen T. V., NguyenT. A.- The Alkaline Resistance of Waterborne Acrylic Polymer/SiO_2 Nanocomposite Coatings. Journal of Analytical Methods in Chemistry, 2022.https://doi.org/10.1155/2022/8266576.
20. Nguyen T. V., Nguyen T. P., Sohrab A., Tran C. D., Hoang D. M., Hoang T. H., Nguyen T. L., Bui T. T. L., Dam X. T., Nguyen N. L., Le T. T., Nguyen T. N. L., Vu Q. T., Tran D. L., Dinh D. A., Le T. L. - The role of organic and inorganic UV-absorbents on photopolymerization and mechanical properties of acrylate-urethane coating, Mater. Today Commun. **22** (2020) 100780.https://doi.org/10.1016/j.mtcomm.2019.100780.
21. Yari H., Moradian S., Tahmasebi N. - The weathering performance of acrylic melamine automotive clearcoats containing hydrophobic nanosilica, J. Coat. Technol. Res. **11** (2013) 351-360.DOI:10.1007/s11998-013-9541-z.
22. Tadele D. M., Zhang C., Liu Y., Diaa E. D. F., Yanli Z. - Surface modification of nano-silica by diisocyanates and their application in polyimide matrix for enhanced mechanical, thermal and water proof properties. Materials Chemistry and Physics **225** (2019) 358-364. https://doi.org/10.1016/j.matchemphys.2018.12.107.
23. Toker R. D., Kayaman A. N., Kahraman M. V. - UV-curable nano-silver containing polyurethane based organic–inorganic hybrid coatings.Progress in Organic Coatings **76** (2013) 1243-1250. https://doi.org/10.1016/j.porgcoat.2013.03.023.
24. Arndt L. W., Junker L. J., Patel S. P., Pourreau D. B., Wang W. - UV-Curable Acrylic Urethane Coatings for Weatherable Applications, Paint án Coatings Industry, 2004.
25. Nguyen T. V., Le X. H., Dao P. H., Decker C., Nguyen T. P. - Stability of acrylic polyurethane coatings under accelerated aging tests and natural outdoor exposure: The critical role of the used photo-stabilizers, Progress in Organic Coatings **124** (2018) 137-146. http://dx.doi.org/10.1016/j.porgcoat.2018.08.013